Bulletin of the Seismological Society of America, Vol. 106, No. 5, pp. 2244–2257, October 2016, doi: 10.1785/0120150249

Encore Ubaye: Earthquake Swarms, Foreshocks, and Aftershocks in the Southern French Alps

by F. Thouvenot, L. Jenatton, D. Scafidi, C. Turino, B. Potin, and G. Ferretti

Abstract The earthquake swarm that took place in 2012–2015 in the Upper Ubaye Valley (the most active seismic zone in the French Alps) is peculiar for two reasons: (1) it occurred a few kilometers from a previous swarm (active in 2003–2004); (2) it was initiated by an M_L 4.3 shock and reactivated, more than two years later, by another M_L 4.8 shock with an identical epicenter but a deeper focus. We present here the corresponding data set of ∼13,000 events, of which ∼3000 were relocated using a double-difference algorithm. The swarm extends north-northwest–south-southeast (N165°E) over a distance of 11 km, but daily snapshots along a 2.5 yr period allow us to identify transverse faults whose activity was often ephemeral. Focal mechanisms for 13 $M_L \geq 3$ events confirm the complexity of the swarm geometry, although the fault plane for the two "mainshocks" is very consistent (N156°E–N160°E strike, 52°–55°SW dip), with clear normal faulting and a slight dextral strike-slip component. Most foci were located in the 4–11-km depth range, within the crystalline basement. Taking into account the source sizes for the two "mainshocks", the hydraulic diffusivity of 0.05 $m^2\,s^{-1}$ found for the 2003–2004 swarm is shown to fit reasonably well the 2012 data, but not the 2014 reactivation sequence. Throughout the article, we discuss the difficult issue of the identification of "foreshocks" and "aftershocks" within such a sequence, even though a swarm, per se, makes this terminology inadequate. As previously suggested by other authors, between a foreshock–mainshock–aftershock sequence and an earthquake swarm also exists a whole gamut of seismic activity which makes this dichotomy much more complex than anticipated.

Introduction

The ∼60-km-long Ubaye Valley stretches from the French–Italian border to the Durance River, itself a left-bank tributary of the Rhone River (Fig. 1). The upper first 30 km of the valley, arguably the most active seismic zone in the French Alps, has long been recognized (Fréchet, 1978; Fréchet and Pavoni, 1979) as the seat of long series of large and small shocks, with no outstanding principal event. This phenomenon of earthquake swarms was first described by Knett (1899) who noticed it in the border region between Germany and the Czech Republic (Vogtland/northwest Bohemia) where it seems perennial, and coined it "Schwarmbeben" (i.e., "swarm quake"). Barani *et al.* (2014) and Scafidi *et al.* (2015) recently pointed out that other swarms frequently occur in the southwestern Piedmont (Italy), in the Stura, Maira, and Varaita Valleys. These valleys which deeply indent the Dora Maira crystalline massif are sited only a few tens of kilometers from Ubaye, an indication that swarms are very frequent on both sides of the border in this part of the French–Italian Alps.

Earthquake swarms are common in volcanic regions such as Japan, central Italy, Afar, or oceanic ridges where they occur before and during eruptions. They are also observed in zones of Quaternary volcanism such as Vogtland/northwest Bohemia (e.g., Hainzl and Fischer, 2002; Horálek and Fischer, 2010) or in intraplate regions (Špičák, 2000). In both cases, fluid migration probably regulates their dynamic evolution, even if this mechanism is more difficult to advance in the case of intraplate regions.

Although at least two hydrothermal sources are documented within a 40 km radius (labels BV and PP in Fig. 1), Ubaye is clearly not a volcanic region. The boundary between Eurasia and the colliding Adriatic microplate, usually likened to the Piedmont seismic arc, lies 40 km to the east (Thouvenot and Fréchet, 2006; Scafidi *et al.*, 2015), but the southwestern Alpine belt is at least 150 km wide, with a moderate seismic activity (typically: three M_L 3 events per year for the whole area corresponding to the French Alps, from Geneva to Nice). Thus Ubaye cannot either be considered a typical intraplate region. Its peculiar seismic activity is rather to be put in relation with the presence of the so-called Embrunais-Ubaye flysch nappes, originally in the core zone of the Alps, which overlapped the external domain owing to

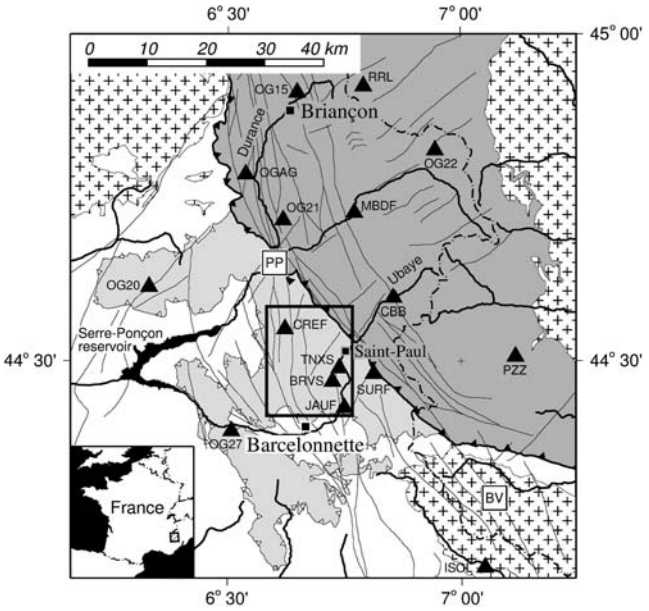

Figure 1. Simplified map of the southwestern Alps, with main geologic features: cross pattern, crystalline massifs (Pelvoux to the northwest, Argentera to the southeast, and Dora Maira to the northeast); light shade, Embrunais–Ubaye nappes; heavy shade, Penninic Domain; heavy barbed line, Frontal Penninic Thrust; faults after Sue (1998). Triangles, seismic stations (Sismalp, Regional Seismic network of Northwestern Italy [RSNI], LDG). Hot springs: PP, Plan de Phasy; BV, Bagni di Vinádio. Dashed line: French–Italian border. Box: study area of Figure 3.

the basement depression between the Pelvoux and Argentera crystalline massifs. For Kerckhove (1969), "the whole history of Embrunais-Ubaye seems to be conditioned by successive [but unsuccessful, our addition] attempts for an external crystalline massif to rise between Pelvoux and Argentera, where it is nowadays lacking". According to the same author, these Upper Cretaceous nappes, mainly made of the schist, limestone, and sandstone series known as *Flysch à Helminthoïdes*, have been in their present place since the end of the Eocene or the middle of the Miocene (20 Ma).

We still do not understand why and how these 1–2-km-thick Embrunais-Ubaye nappes can nurture earthquake swarms in the underlying crystalline basement, but it is a fact that most earthquakes occur there at depths larger than 4 km (relative to sea level). If we take into account a mean elevation of 1–2 km, a value close to the nappe thickness itself, and a 1–2-km-thick parautochthonous Mesozoic series (Kerckhove *et al.*, 1978), this seismic activity reveals the stress which prevails in the pre-Triassic basement, much more than in the nappes themselves, whose current mobility is unknown, or in the underlying Mesozoic series. Normal-faulting mechanisms with an extension direction perpendicular to the general trend of the Alps show moreover that postcollisional tectonics are now the rule in this area (Sue, 1998; Sue *et al.*, 1999).

The upper Ubaye Valley was the seat in 2003–2004 of a profuse earthquake swarm whose 16,000 event corresponding sequence was studied in detail by Jenatton *et al.* (2007) from the inception of the phenomenon till its fading, and revisited by Daniel *et al.* (2011) and Leclère *et al.* (2013). After a brief review of these studies, we will present what occurred 10 yrs later in 2012–2015, when an M_L 4.3 earthquake struck ~6 km northwest from the 2003–2004 swarm; this earthquake soon bred another swarm, more complex than the first one. That swarm was still active, more than two years later, when another M_L 4.8 shock struck exactly at the same place as the M_L 4.3 event, instantaneously reactivated the swarm, and thereafter extended the active zone by 5 km toward the northwest. This swarm–earthquake interaction and mutual triggering bring into question the identification of "foreshocks" and "aftershocks" within a swarm. We will discuss this issue and try to demonstrate that the distinction usually taken for granted between a foreshock–mainshock–aftershock sequence and earthquake swarms is much more complex than anticipated. A whole gamut exists between these two classes, which means, for instance, that in the Alps (or elsewhere in the world) one can very often observe an isolated doublet of two events with equivalent magnitude, which can be considered the poor relation of the earthquake swarm family.

Previous Seismic Activity

To account for the shift between the two swarms, the present study area (44°25′N–44°35′N and 6°35′E–6°46′E) is slightly shifted to the northwest of the 2003–2004 study area of Jenatton *et al.* (2007). Both areas approximately cover 270 km^2, which is convenient for comparisons; they also encompass the epicentral zone of one of the two or three largest earthquakes in the French Alps in the last century (5 April 1959, M_w 5.5). As stated by Jenatton *et al.* (2007), the corresponding horizontal uncertainty for the 1959 event is probably large (at least 10 km): although the macroseismic epicenter is clearly Saint-Paul (Fig. 1), some instrumental relocations shift the epicenter to Barcelonnette, 17 km to the southwest, on the southern fringe of the present study area. The focal solution computed by Fréchet (1978) shows a right-lateral strike-slip motion along an N175°E-striking plane, with a small extensional component. Jenatton *et al.* (2007) also list a number of swarms studied by Fréchet (1978), Fréchet and Pavoni (1979), and Guyoton *et al.* (1990), which shows that Ubaye, besides being prone to the classical mainshock–aftershocks sequence such as the 1959 event, is much more frequently liable to earthquake swarms.

In the remaining part of their study, Jenatton *et al.* (2007) describe what remains, to present day, the most prolific of these swarms. It took place in 2003–2004 and, although only about one tenth of the shocks was precisely relocated, the complete time series includes more than 16,000 events, with magnitude values as low as −1.3. The activity began in January 2003, reached its climax in October 2003 with three M_L 2.7 shocks, and is somewhat arbitrarily limited to December 2004, albeit a few more low-magnitude shocks occurred all through 2005. The activity was shown to cluster along a 9-km-long, 3- to 8-km-deep rupture zone which trends N145°E across

the valley and dips 80°SW. Focal mechanisms for the larger shocks show either normal faulting with a southwest–northeast-trending extension direction or northwest–southeast strike slip with right-lateral displacement. The activity initiated in the central part of the rupture zone, diffused to its periphery, and eventually concentrated in its southeastern deeper part where the late 2005 shocks are also to be found; the corresponding hydraulic diffusivity is about 0.05 $m^2\,s^{-1}$. The Gutenberg–Richter *b*-value significantly varied between 1.0 and 1.5 in the course of the phenomenon.

Daniel *et al.* (2011) revisited this ∼16,000 event sequence and studied changes in effective stress (normal stress minus pore pressure). They hypothesized that background events were directly triggered by pore-fluid pressure changes at depth. Then, using rate-and-state constitutive friction laws, they estimated changes in effective stress. The maximum change is close to −8 MPa, which corresponds to a maximum fluid overpressure of about 8 MPa under constant normal stress conditions. This estimate is in good agreement with values obtained from numerical modeling of fluid flow at depth, or with direct measurements reported from fluid injection experiments.

More recently, Leclère *et al.* (2013) provided additional constraints on the temporal and spatial changes in fluid overpressure. Using an extended set of 74 focal solutions spanning the whole 2003–2004 Ubaye episode, they showed that the fluid overpressures required to reactivate the cohesionless fault planes vary through time, with values close to 35 MPa at the inception of the swarm, an increase up to 55 MPa during the activity climax and a final decrease down to 20 MPa. For these authors, fluid overpressures are developed along two parallel faults bordering a pull-apart-like, releasing bend structure, the interior of which is characterized by low to null overpressure. Creep compaction could be the process allowing these features and the observed migration of seismicity.

Data and Processing

The active zone of the 2012–2015 swarm is centered on the Parpaillon massif, a watershed between the upper Ubaye Valley (Alpes-de-Haute-Provence) and the Embrunais subregion (Hautes-Alpes). Since 1989, the seismic activity of this area has been monitored by Sismalp, a 40-station seismic network spread over the French Alps, from the Lake of Geneva to Corsica, and by adjacent seismic networks in Italy and France. Although Sismalp stations were primarily equipped with 1 Hz seismometers and recorded only triggered windows, four stations (2 French and 2 Italian) located in the frame of Figure 1 now continuously transmit real-time broadband signals to Grenoble and Genoa. They are included in a set of about 20 broadband stations in the French, Italian, and Swiss Alps. In particular, stations belonging to the Regional Seismic network of Northwestern Italy (RSNI; Scafidi *et al.*, 2015) better constrain hypocentral coordinates and focal mechanisms.

Two permanent Sismalp stations (CREF and JAUF) are located in the study area shown by the box in Figure 1. They were supplemented in 2012–2013, and again in 2014–2015, with two temporary stations (BRVS and TNXS) implanted as close as possible to the earthquake swarm (epicentral distances in the 0.6–15 km range); both stations were installed a few days after the February 2012 and April 2014 shocks that respectively initiated and reactivated the swarm. All four stations provide only triggered signals, just as ∼60% of the stations in the area covered by Figure 1. In this area, the network was practically kept unchanged between 2003 and 2015, except for station SURF (triggered, short-period, vertical-component signals in 2003 versus continuous, broadband, three-component recording as of 2006). The sampling frequency is 100 Hz everywhere.

Seismograms were manually picked and earthquakes prelocated with the PICKEV2015 software (see Data and Resources), which enables an interactive control of picked arrivals. A preliminary catalog of hypocenters was then built up using HYPREF2015, a modified version of the HYPO71 program (Lee and Lahr, 1975) which takes second arrivals and station altitudes into account (see Data and Resources). All focal depths are referred to sea level. M_L magnitude values are those computed by Sismalp by applying Richter's original technique. When the moment magnitude M_w can be computed by other agencies (usually for $M_L > 3.5$ events), M_w values and Sismalp M_L values are found to be consistent within about 0.1 (Sira *et al.*, 2012, 2014; Cara *et al.*, 2015).

We eventually formed travel-time differences from *P* and *S* picks with the PH2DT program (Waldhauser and Ellsworth, 2000; Waldhauser, 2001), and used their hypoDD program to improve location precision. Only stations situated within a distance of 150 km were used. Links built for each event were limited to a maximum number of 50 neighboring events within a search radius of 20 km. To reach this maximum number, only strong neighbors with more than eight phase pairs were considered; other neighbors were selected, but not counted as strong neighbors. To prevent the number of links from becoming too large, we restricted them to 100 for each event pair. With these limitations, the number of processed events is reduced from ∼6000 to ∼3000, and the amount of data remains acceptable (∼1,500,000 *P*-arrival pairs and ∼1,300,000 *S*-arrival pairs).

We first jointly relocated the 2003–2004 and 2012–2015 swarms. But when the activity of the second one developed, we decided to suppress data for the first one, which allowed us to include a larger number of relocated events in the 2012–2015 dataset. Before doing that, we checked that the relative position of both swarms was consistent.

The velocity model used is borrowed from Sellami *et al.* (1995): this is an 8-layer crustal model starting from 4.85 $km\,s^{-1}$ at the surface, and where the 6 $km\,s^{-1}$ velocity is reached at 10 km. We preferred manual picks to waveform correlations because we tried the latter technique when processing the 2003–2004 swarm, and found that it did not clearly improve results when the swarm is several kilometers long and waveforms vary (compare Jenatton *et al.*, 2007, with Daniel *et al.*, 2011). In the present study, the whole seis-

mic activity is therefore relocated as a single cluster. Location might be further improved if the swarm were subdivided into several clusters, as other coming studies will try to demonstrate.

Sequence of the 2012–2015 Earthquake Swarm

In the following, although we frequently compare the 2003–2004 swarm to its 2012–2015 counterpart, we do not present the activity of the 2005–2011 period. Of course we checked and studied it, but found, just as Jenatton *et al.* (2007) did for the 1989–2002 period, that it mainly consisted of scattered epicenters with no obvious link to the swarm under study.

In January and February 2012, CREF and JAUF stations, respectively 7 and 10 km to the north-northwest and to the southeast of the 2012–2015 swarm, detected every two days one or two (usually nonlocatable) events with an *S–P* smaller than 1.5 s, which can be considered the background activity of the area. The activity slightly increased on 24 and 25 February 2012 (4 events per day), just before the M_L 4.3 earthquake one day later. The foreshock nature of this activity will be discussed at the end of this section.

The macroseismic effects of the 26 February 2012 M_L 4.3 earthquake (henceforth denoted EQ1) are described by Sira *et al.* (2012). Damage was slight, with a maximal European Macroseismic Scale 1998 (EMS98) intensity V–VI ascribed to three localities: La Condamine-Châtelard (8 km from the epicenter); Jausiers (10 km); and Barcelonnette (12 km). All three localities are situated in the upper Ubaye Valley, where a site effect due to glacial sedimentation can be expected, especially for Barcelonnette, the largest town in the valley. The earthquake was much more distinctly felt to the south than to the north. This was quantitatively confirmed in Nice and Grenoble, two cities situated at ~100 km from the epicenter: for similar site conditions, ground-motion measurements were eight times larger in Nice than in Grenoble. Courboulex *et al.* (2013) discuss these peculiar effects of rupture directivity.

Figure 2 shows the complete time series for the ~13,000 events detected by the closest stations, and the ~6000 events that could be located using the HYPREF2015 standard location code. The smallest magnitude was measured at −0.8, but such rare events with negative magnitudes are not shown in this figure. The cutoff magnitude is about 0.5. The maximal number of events daily detected (455 in less than 5 hrs) was reported on 7 April 2014 when the M_L 4.8 event (henceforth denoted EQ2) took place. The corresponding hypocenter is practically the same as for EQ1, with only a slight shift to the south (~300 m), and a somewhat larger focal depth (9.9 versus 8.8 km). Damage was heavier than for EQ1 (Sira *et al.*, 2014), and a maximal EMS98 intensity of VI was this time ascribed to the same three localities listed above (La Condamine-Châtelard, Jausiers, and Barcelonnette). The directivity effects described by Courboulex *et al.* (2013) for EQ1 were not observed as distinctly for EQ2.

Over the next 3 or 4 days, the daily seismicity rate kept above 200, a value which had only been reached once in February 2012. Table 1 is an attempt to recognize different phases in the histogram of Figure 2. Figure 3 (left) shows the ~3000 epicenters relocated using hypoDD. Although on this kind of representation the 2012–2014 events (light shade) are almost completely obliterated by posterior events (heavy shade), the swarm seems at first glance much more complex than its 2003–2004 counterpart, whose northwestern tip shows up in the lower right corner of the figure. It has a rather similar trend (N165°E versus N145°E for 2003–2004), a similar length (11 versus 9 km), but it is definitely much more solid (5 km versus 1.5 km in width). Figure 3 (right) shows the same catalog as Figure 3 (left) except that symbol size does not take magnitude into account. This allows us to better ascertain the general trend of the swarm (N165°E), and also to reveal transverse features trending southwest–northeast, which contribute to its complexity. One can also note in Figure 3 (right) that the southwestern boundary of the swarm is sharply defined, as if cut with a knife, whereas its northeastern boundary is much more diffuse.

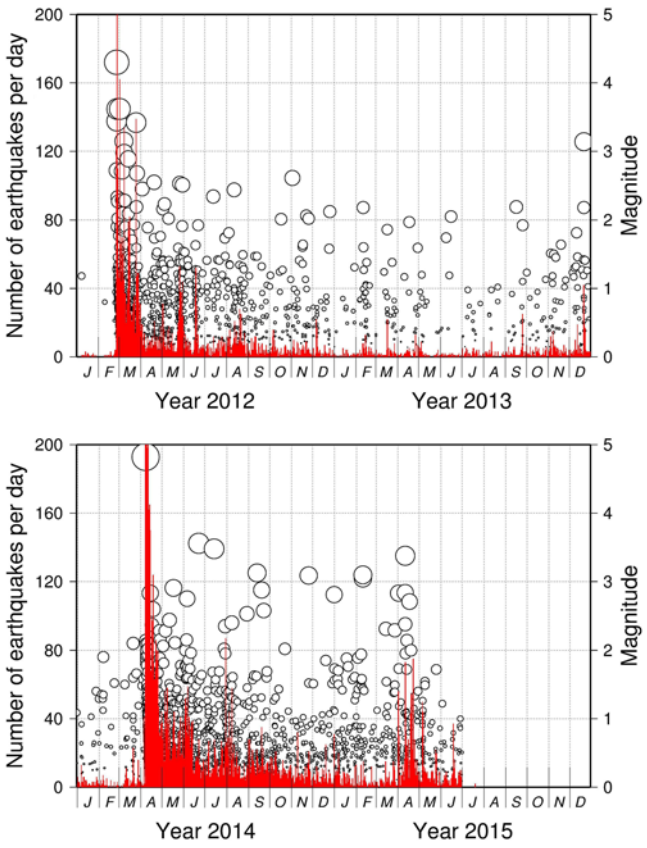

Figure 2. Complete time series for the ~13,000 events detected during the 2012–2015 earthquake swarm, and the corresponding ~6000 events located. The color version of this figure is available only in the electronic edition.

Cross sections (Fig. 4) show that the swarm is located between 4 and 11 km at depth, that is to say in the crystalline basement, even for its upper part. Along strike as well as across, the swarm is divided into two parts. Along strike (Fig. 4, top left), events to the northwest of the two "mainshocks" are less dense, as already noticeable from the maps of Figure 3.

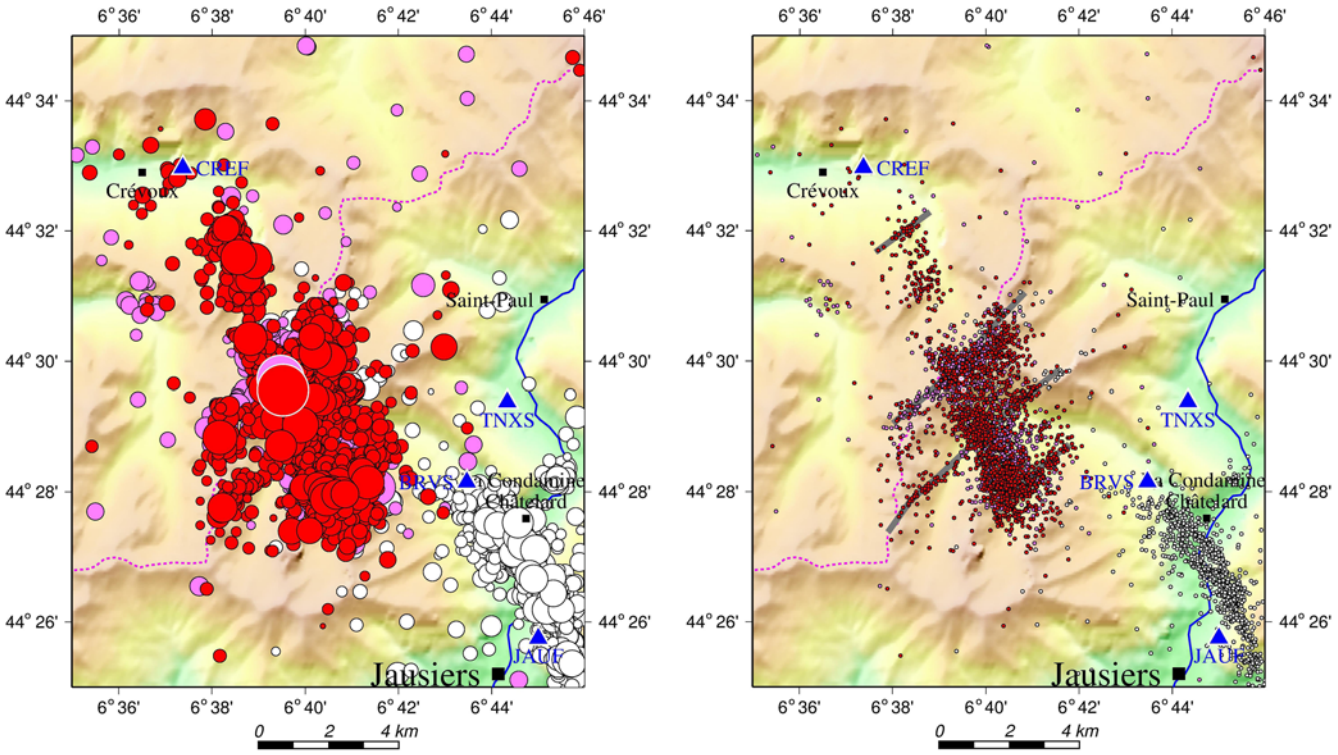

Figure 3. Double-difference locations for earthquakes in the study area: (left) light shade: 1 January 2012 to 6 April 2014, heavy shade: 7 April 2014 to 30 June 2015, white: 2003–2004 for comparison; epicenters of EQ1 and EQ2 (the two 2012 and 2014 "mainshocks") shown respectively by light-shaded and heavy-shaded disks with white outline; (right) same as (left), but with symbol size not scaled on magnitude, to emphasize southwest–northeast transverse faults. Triangles, seismic stations in the study area. Topography from Shuttle Radar Topography Mission (SRTM) data. The color version of this figure is available only in the electronic edition.

These events, which mainly occurred after EQ2, delineate a feature in the 6–11-km-depth range, separated from the main part of the swarm by a kind of gap. Across the swarm (Fig. 4, bottom left), the most obvious feature is a rather bulky, 4–11-km-deep patch which dips at ~70°SW, and in the lower part of which EQ1 and EQ2 are found. This dip value is consistent with the 80°SW dip found by Jenatton *et al.* (2007) for the 2003–2004 swarm. A shallower patch in the 4–7-km-depth range also complicates the geometry to the southwest. It is to be put in relation with transverse faults across the swarm, whose activity would thus be limited to this depth range.

Figure 4 (right) shows activity in the 12 hrs following EQ1 and EQ2. We hypothesize that those early events better demonstrate the relative position of the two rupture zones, as discussed later. EQ1, EQ2, and these early aftershocks were located using exactly the same set of permanent stations. (The temporary stations BRVS and TNXS were installed or reinstalled a few days after EQ1 and EQ2 occurred.) We therefore believe that the 1 km difference in depth between EQ1 and EQ2, as well as that of their respective early aftershocks, is significant.

Some events, on the map as on cross sections, are obviously unrelated to the swarm and belong to the background seismicity of the area. This is especially the case for an isolated M_L 2.0 event (best seen in Fig. 4, bottom left) which occurred in late 2014 close to Saint-Paul, the only event with a magnitude reaching 2 located in the study area which has no connection with the swarm. At an atypical depth of 3 km and separated from the swarm by 2.5 km, this event is probably not the sole one related to the background seismic activity (another is 2 km farther north, see map Fig. 3 left).

Figure 5 emphasizes the tendency for large-magnitude earthquakes to occur deeper in the crust. For each magnitude value increasing from 0 to 5 with a 0.05 step, the bold line links the shallowest depth value found in the catalog.

The issue of location precision can be addressed by means of the "foreshock" activity just before the two "mainshocks". Our quotes point to the impropriety to dub foreshocks and mainshocks events which are part of an earthquake swarm, an archetype from which mainshocks are precisely absent. Table 2 suggests that some activity took place in the couple of days preceding EQ1 and EQ2. This is perhaps more conspicuous for 2012, when five events occurred in less than 4 days in the vicinity of EQ1. Out of these five events, the last two occurred 26 and 21 hrs before, and their epicenters are very close to that computed for EQ1, thus providing a horizontal uncertainty of a few tens of meters only if we assume that the two "foreshocks" pinpoint the "mainshock" nucleation. There is, however, a discrepancy of ~800 m in focal depth.

Except for two isolated events which occurred in early January and early February on the fringe of our study area, hence probably corresponding to background seismicity, these five "foreshocks" were the sole events we could detect.

Table 1
Swarm Chronology

Phase	Period (yyyy/mm/dd)	Maximum M_L	Average Daily Rate	Comments
A	2012/01/01–2012/02/22	1.2	0–1	Background activity
B	2012/02/23–2012/02/26	1.0	3	Foreshock activity
C	2012/02/26–2012/03/31	4.3	60	M_L 4.3 (EQ1) followed by five $M_L > 3$ events. Maximum daily rate: 221 (27 February 2012)
D	2012/04/01–2013/04/30	2.6	6	Activation of the swarm and migration to the southeast
E	2013/05/01–2013/08/31	2.1	1–2	Four months of very low activity. May 2013: no $M_L > 1.2$. June 2013: three events detected per day, the lowest rate observed since the inception of the crisis. July–August 2013: no $M_L > 1.0$
F	2013/09/01–2013/12/31	3.1	4	Four months of higher activity, with an unexpected M_L 3.1 in December 2013
G	2014/01/01–2014/03/08	1.9	2	Low activity
H	2014/03/09–2014/04/06	2.1	6	Slight activity increase
I	2014/04/07–2014/04/30	4.8	133	M_L 4.8 (EQ2) followed by NO $M_L > 3$ event, but by 3186 low-magnitude events which instantaneously reactivated the whole swarm
J	2014/05/01–2015/03/31	3.6	13	Steady-state activity within the whole swarm, with six $M_L > 3$ events in 11 months
K	2015/04/01–2015/05/31	3.4	20	Two months of higher activity: 73 events detected on 11 April 2015, M_L 3.4
L	2015/06/01–2015/06/30	1.2	10	Low activity, but with an average daily rate still much larger than the background-activity level in A

For a similar 4 day period, we found that EQ2 has also been preceded by a 5-event sequence (Table 2). But naming them "foreshocks" is questionable, because at that time the swarm was still active (it had been active for more than two years almost discontinuously), and locations in Table 2 do not show a consistency similar to that we found for EQ1. Unless our location accuracy degraded with time between 2012 and 2014, an eventuality difficult to accept, we prefer to consider this activity prior to EQ2 as linked to the steady-state regime of the swarm, and not to some precursory phenomenon. However, the 4 April event in Table 2 as well as the two other 7 April events have their epicenters within ~600 m from EQ2, which is still consistent with the fault size for an M_L 4.8 earthquake to make them "foreshocks".

Migration of Seismic Activity

Dynamics of an earthquake swarm can be complex to present. In Figure 6, we selected nine snapshots over a period of 31 months (1 January 2012 to 31 August 2014). Each snapshot shows, in a shade scale ranging from black (day 0) to a very light shade (day 17), epicenters in the 18 days preceding and including the title date. Events older than 17 days are shown in white (see Data and Resources for accessing the film these snapshots are taken from).

The first snapshot (24 February 2012) shows in black the two precursors that occurred 2 days before EQ1. (In all snapshots, two white circles show the epicenters of EQ1 and EQ2.) Two other events on the fringe of the map reveal the background seismic activity in early January and early February 2012, as discussed in the previous section.

Snapshot 27 February 2012 shows epicenters in the first 24 hrs after EQ1. They delineate a 2-km-long segment typical for an M_L 4.3 shock, and might therefore be considered as proper aftershocks. If we hypothesize that such an activity shows where rupture actually took place, the location of EQ1 at the northwestern tip of this segment suggests a unilateral rupture, from northwest to southeast.

In snapshot 10 March 2012, the swarm geometry becomes more complex, especially with the appearance of a 3-km-long transverse southwest–northeast lineament along the watershed between Ubaye (to the southeast) and Embrunais (to the northwest). Twelve days later (snapshot 22 March 2012), this lineament was still active and the swarm then began a steady growth toward the southeast.

Nearly one year later (snapshot 21 December 2013), the swarm has practically reached its final geometry shown in Figure 3. Its southern tip was reactivated on 21 December 2013 by an unexpected M_L 3.1 shock which occurred close to the bayonet separating the present swarm from the 2003–2004 swarm.

Snapshot 6 April 2014 shows the situation just before EQ2. As discussed in the previous section, the swarm was then still active in different places, whereas at least two events (foreshocks?) occurred in the vicinity of the "mainshock" to come. This epicentral zone, in the northern part of the swarm, has been kept almost continuously active since the inception of the crisis (compare with the previous five snapshots).

In the 4.5 hrs that followed EQ2 (snapshot 7 April 2014), the swarm was instantaneously reactivated over a length of ~4 km, again a reasonable rupture size for an M_L 4.8. Just as for EQ1, we hypothesize that the location of EQ2 at the northwestern tip of this segment again suggests a unilateral rupture from northwest to southeast. This activity continued the next day (snapshot 8 April 2014), with the addition, farther to the northwest, of a subswarm separated by a 3 km gap. It

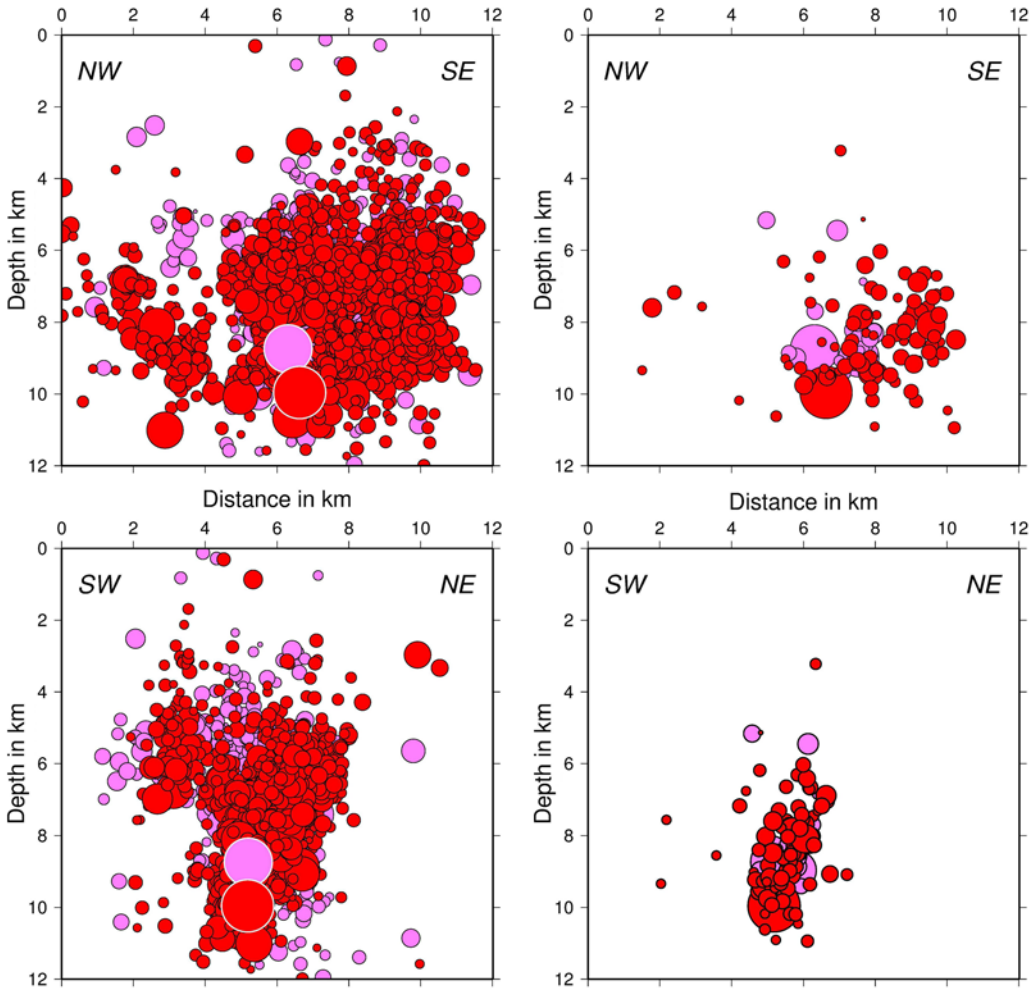

Figure 4. (Left) Sections across the 2012–2015 earthquake swarm (double-difference locations), along the N165°E direction (top) and along the perpendicular N75°E direction (bottom). Same shade codes as in Figure 3. Midpoint on the distance axis (6 km) is 44°30′N–6°40′E. Depth referred to sea level. (Right) Same sections, showing only events which occurred in the first 12 hrs after EQ1 and EQ2. The color version of this figure is available only in the electronic edition.

shows that EQ1 and EQ2, although seemingly similar, occurred in different contexts regarding stress distribution.

This gap was partially filled 2 months later (snapshot 3 June 2014), leaving two subgaps on both sides. One of these subgaps was subsequently filled in February 2015; the other is still vacant at the time this article is written (see Fig. 3, left). The complicated history of this zone, much less active than the main swarm, can be better analyzed in Figure 7, which displays a vertical chronology of the along-strike activity (see the left side of the figure between April 2014 and July 2015).

Figure 7 also shows that, month after month, the initial 2-km-long 2012 rupture has been slowly but steadily extended in the southeast direction to reach 4.5 km in length 1 year later. To the northwest of EQ1, the same kind of migration occurred over a distance of 1 km only.

For the 2003–2004 swarm, Jenatton *et al.* (2007) showed that the radius of the active zone clearly did not increase linearly with time, but was governed by a diffusion law. The hydraulic diffusivity

$$D = \frac{r^2}{4\pi t}$$

that links radius r to time t (e.g., Shapiro *et al.*, 2002) was found to be of the order of 0.05 $m^2\,s^{-1}$. We tried in Figure 8 to compare diffusion laws for three data sets: the 2003 swarm (top), the activity after EQ1 (center), and after EQ2 (bottom). For each hypocenter, distance is computed from the first $M_L > 1$ event (top); from EQ1 (center); and from EQ2 (bottom). We found that the $D = 0.05$ $m^2\,s^{-1}$ parabola indeed fitted the diffusion in the first case. For EQ1, it obviously does not, except if this parabola is shifted by ∼1.5 km, a value which roughly corresponds to the rupture length for an M_L 4.3 event (see parabola marked 0.05* in Fig. 8, middle). For EQ2, although a similar shift by ∼3 km could hardly account for the diffusion in the first half of the time series, it fails in the second half. There is clearly a different behavior between the 2012 activity, more similar to the 2003 swarm, and the 2014 activity that shows no diffusion at all.

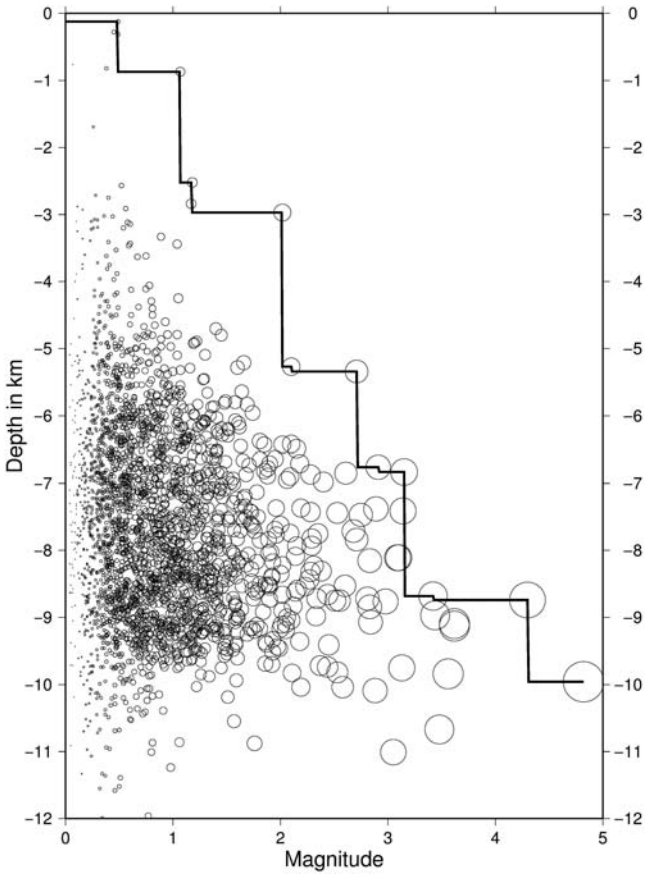

Figure 5. Depth–magnitude distribution (double-difference locations). Bold line links, for a magnitude value increasing from 0 to 5 with a 0.05 step, the shallowest depth value found in the catalog. Depth referred to sea level.

Focal Solutions

Using the program FPFIT (Reasenberg and Oppenheimer, 1985), we computed 13 focal mechanisms (Fig. 9 and Table 3) for $M_L \geq 3$ events, all in the same depth range (7–11 km). For most of them, we used only polarities read on Sismalp and RSNI stations; for EQ1 and EQ2 (labels 1 and 8), we took into account as many readings as possible, using especially the Résif and LDG networks (France), but also other Italian stations, and the Swiss network. Thus, albeit the average number of polarities is close to 40 for most focal solutions shown here, EQ1 and EQ2 count respectively ~70 and 150 polarities.

Actually, two additional events should have been included: (1) on 15 February 2015, two M_L 3.1 events occurred 13.5 s apart, but we could not read enough reliable polarities for the second one; (2) on 11 April 2015, an $M_L \sim 2.7$ event occurred only 0.72 s before an M_L 3.4 event, which also makes impossible the analysis of this latter.

Even so, the 13 remaining mechanisms are not all well constrained, especially those corresponding to pure normal faulting (labels 2–4, 7, and 12). In that case, the direction of the *T* axis varies by several tens of degrees, although keeping a northwest–southeast trend. The other focal solutions split into two groups: (1) strike-slip mechanisms (labels 5 and 6), with what we assume to be the fault-plane striking ~N135°E; (2) normal-faulting mechanisms with a slight strike-slip component (labels 1, 8–11, and 13). This latter group includes EQ1 and EQ2, which have similar though not identical mechanisms (N156°E–N160°E strike, 52°–55°SW dip, again for what we assume to be the fault plane).

Note that, in the map shown at the bottom of Figure 9, the different events studied here do not group according to their mechanisms, although events 2–4 (pure normal faulting) have very close epicenters. Event 13, the only $M_L > 3$ event in the much less active northwestern part of the swarm, has a mechanism rather similar to the others, except perhaps a more north–south-striking fault plane.

Discussion and Conclusions

The most striking feature of the protracted seismic activity observed in Ubaye from 2012 to 2015 is the occurrence, more than 2 years apart, of two M_L 4.3 and 4.8 shocks

Table 2
Foreshock Activity in 2012 and 2014

Date (yyyy/mm/dd)	Origin Time (UTC) (hh:mm:ss)	N Latitude	E Longitude	*Z* (km)	M_L	Number of Phases*	Δ (km)†
2012/02/23	*10:54:31*	*44°30.0′*	*6°40.3′*	*6.0*	*0.5*	*6*	*1.10*
	18:44:17	*44°30.4′*	*6°40.9′*	*6.4*	*0.3*	*6*	*2.20*
2012/02/24	19:13:51	44°29.84′	6°39.68′	8.36	0.8	27	0.28
	20:24:59	44°29.75′	6°39.52′	7.93	1.0	29	0.01
2012/02/26	01:21:56	44°29.78′	6°39.51′	8.08	0.6	8	0.06
	22:37:56	**44°29.75′**	**6°39.51′**	**8.80**	**4.3**	**50**	**0**
2014/04/03	23:45:45	44°29.37′	6°38.12′	6.45	0.6	8	1.95
2014/04/04	13:35:37	44°29.44′	6°39.70′	8.98	1.6	32	0.33
2014/04/05	14:44:23	44°27.79′	6°40.49′	6.40	0.4	8	3.56
2014/04/07	12:54:38	44°29.34′	6°39.64′	8.42	0.3	13	0.48
	17:23:00	44°29.63′	6°39.12′	8.94	0.5	11	0.59
	19:26:59	**44°29.59′**	**6°39.56′**	**9.94**	**4.8**	**51**	**0**

Italic: HYPREF2015 standard location; roman: hypoDD double-difference location; bold roman: EQ1 and EQ2 (mainshocks).
*The number of arrival times used for locating the event.
†The horizontal distance between the current epicenter and that of EQ1 (upper part of the table) or EQ2 (lower part).

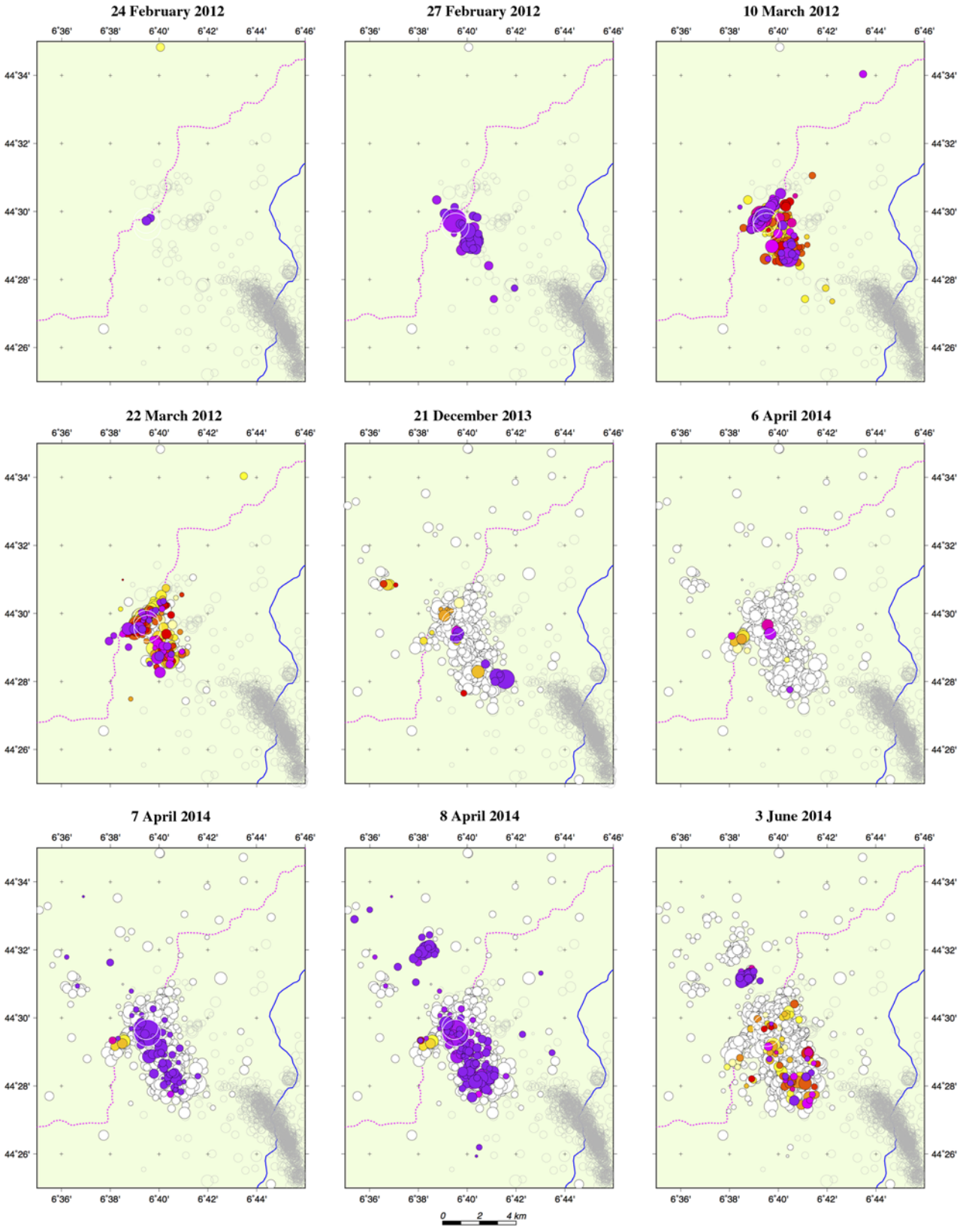

Figure 6. Nine snapshots selected over a period of 31 months (1 January 2012 to 31 August 2014). Each snapshot shows in a shade scale ranging from black (day 0) to a very light shade (day 17) epicenters in the 18 days preceding and including the title date. Events older than 17 days are shown in white. In all snapshots, two white circles show the epicenters of EQ1 and EQ2 (the two "mainshocks"). Light gray circles show activity during the 2003–2004 swarm. See Data and Resources for accessing the film these snapshots are taken from. The color version of this figure is available only in the electronic edition.

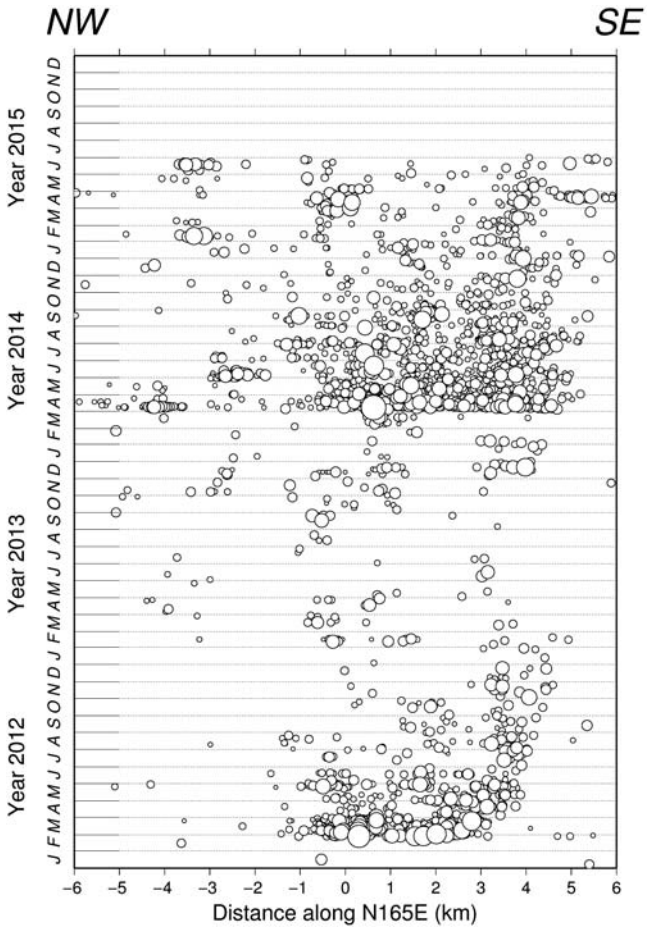

Figure 7. Migration of the activity during 2012–2015. Distance axis trends N165°E, with an origin in 44°30′N–6°40′E.

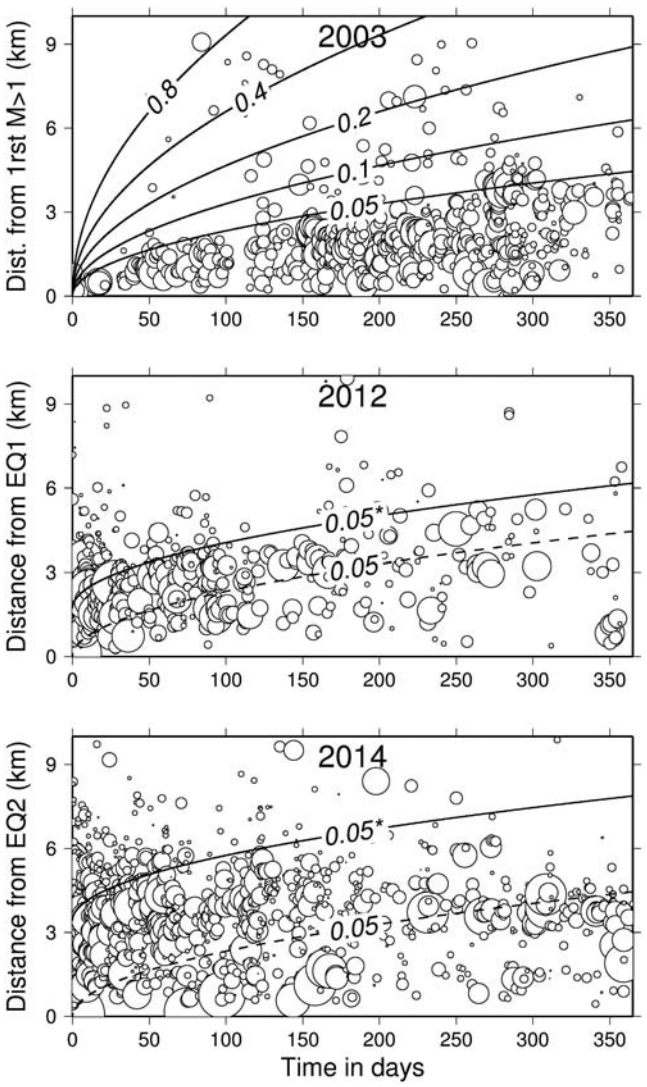

Figure 8. Comparison of the diffusion process for three data sets: (top) 2003 swarm; (middle) 2012 seismic activity; and (bottom) 2014 reactivation. For each hypocenter, distance is computed from the first $M > 1$ shock (top); from EQ1; and from EQ2 (bottom). Diffusion parabolas computed for different diffusivity values (in $m^2 s^{-1}$). See text for full discussion.

(EQ1 and EQ2) with identical epicenters (within 300 m in latitude and 70 m in longitude). Both focal mechanisms (normal faulting with an east–west tension axis, and a slight strike-slip component) are similar though not identical. Of course, the two shocks could be explained by slip on two different conjugate fault planes, but early aftershocks (triggered in the first few hours) clearly show in Figure 6 that the same fault segment was involved (N165°E strike).

The only difference lies in the focal depth (8.8 versus 9.9 km) and this could point to a deeper fault area in the second case. On cross sections showing early aftershocks (Fig. 4, right), the fault area has a length of ∼2 km and a width of ∼1 km at a depth of ∼8.5 km for EQ1. It is 4 by 1 km for EQ2, deeper in its northwestern end (∼10 km) where the two "mainshocks" were situated, and shallower (∼7 km) in its southeastern end which was not ruptured by EQ1. Slip on such a 4-by-1-km fault geometry is anyway consistent with an $\sim M_L$ 5 earthquake. Thus, if EQ1 and EQ2 have identical epicenters, a deeper patch was ruptured in the second case, with a fault length twice as long. Maps of early aftershocks in Figure 6 show that the two epicenters of EQ1 and EQ2 are located at the northwestern tip of the active segment. We hypothesize that, in both cases, rupture was unilateral, with a propagation toward the southeast. A study of high-frequency directivity effects led Courboulex *et al.* (2013) to recognize this for EQ1.

We also demonstrated the general tendency for large magnitudes to occur at larger depths. In the 2003–2004 sequence, which we consider a typical swarm, larger shocks ($2.0 \le M_L \le 2.7$) were instead found around 6 km, right in the middle depth range of the 3–8-km-deep rupture zone, and not deeper. This could well be an interesting difference between typical and atypical swarms which would require further investigation in swarm literature.

We had the rare opportunity to observe foreshocks of low magnitude (between 0.3 and 1.0) up to 3 days before EQ1. Their epicenters and that of the mainshock almost coincide. Although foreshock activity was also observed

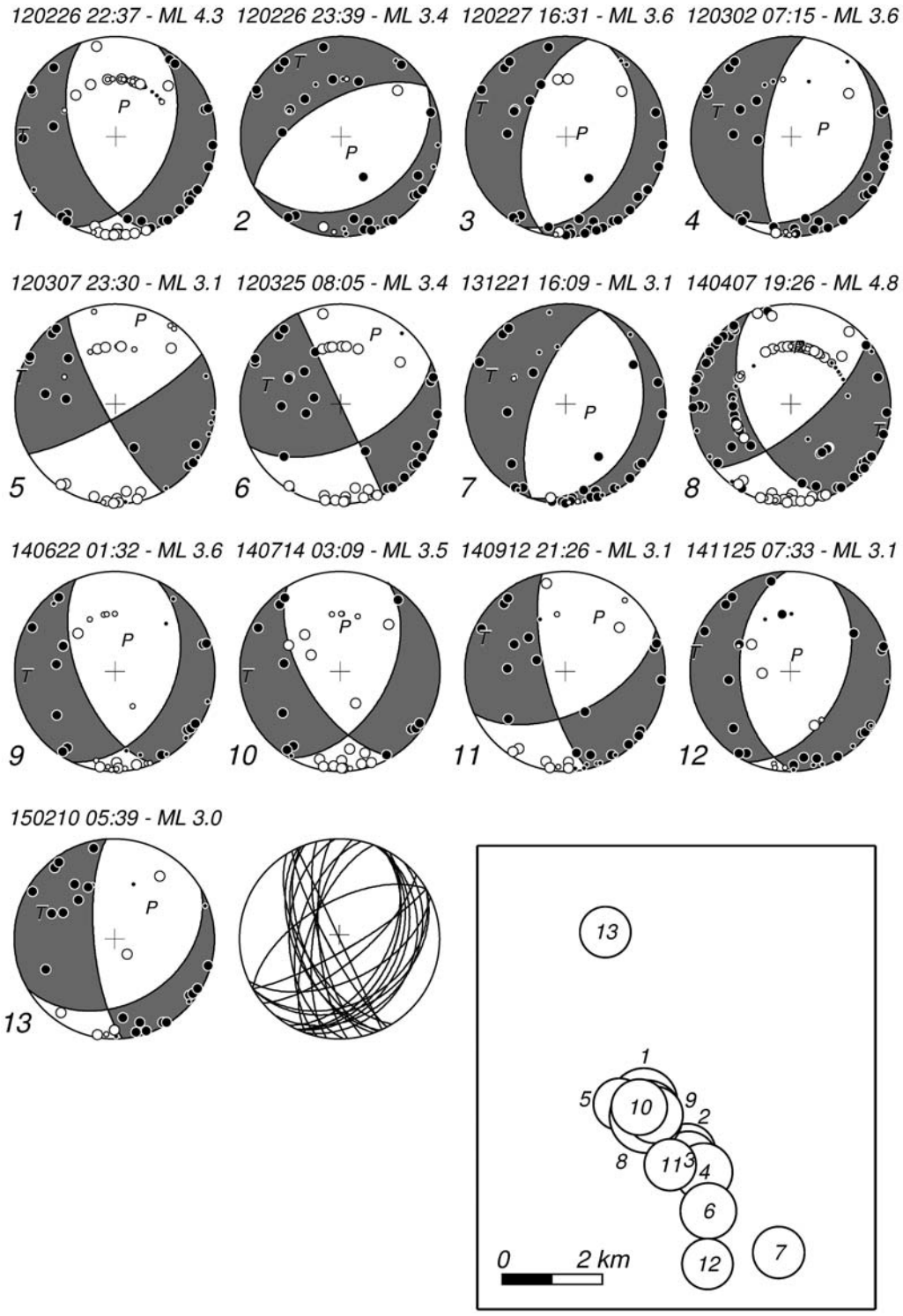

Figure 9. Focal mechanisms (lower hemisphere, equal-area projection) for 13 $M_L > 3$ events of the earthquake swarm. Heading over each diagram reads date, origin time, and magnitude. Compressions shown by full circles; dilatation by open circles; small circles are less reliable polarity readings.

prior to EQ2, it was not focused in the same way, because the swarm triggered in 2012 by EQ1 was still active in 2014 when EQ2 occurred.

The N165°E trend of the present swarm is close to that found by Jenatton *et al.* (2007) for the 2003–2004 swarm (N140–N150°E). These authors suggested a link between Ubaye and northwest–southeast-striking faults in the Argentera massif (Fig. 1). This idea was revived by Sanchez *et al.* (2010) who involved their newly mapped, northwest–southeast-striking fault connecting Ubaye to Argentera (Jausiers–

Table 3
Focal Mechanism Parameters for the 13 $M_L \geq 3$ Events Studied Here

Origin Time (UTC) (yyyy/mm/dd hh:mm:ss)	N Latitude	E Longitude	Z (km)	M_L	Strike (°)	Dip (°)	Rake (°)	NOBS	STDR	F
2012/02/26 22:37:56	**44°29.7′**	**6°39.5′**	**8.8**	**4.3**	**160**	**55**	**−120**	**72**	**0.58**	**0.05**
2012/02/26 23:39:35	44°29.2′	6°40.2′	8.9	3.4	60	30	−90	40	0.66	0.08
2012/02/27 16:31:21	44°29.1′	6°40.2′	9.0	3.6	25	35	−80	40	0.55	0.06
2012/03/02 07:15:51	44°29.0′	6°40.4′	9.0	3.6	40	25	−60	40	0.52	0.08
2012/03/07 23:30:19	44°29.7′	6°39.1′	6.7	3.1	60	80	−10	43	0.77	0.04
2012/03/25 08:05:31	44°28.6′	6°40.5′	8.5	3.4	65	55	0	46	0.66	0.02
2013/12/21 16:09:22	44°28.1′	6°41.5′	7.2	3.1	20	25	−90	38	0.49	0.10
2014/04/07 19:26:59	**44°29.6′**	**6°39.6′**	**9.9**	**4.8**	**50**	**70**	**−40**	**149**	**0.69**	**0.11**
2014/06/22 01:32:15	44°29.6′	6°39.7′	9.8	3.6	25	40	−50	39	0.53	0.03
2014/07/14 03:09:25	44°29.7′	6°39.4′	10.6	3.5	30	50	−40	33	0.48	0.03
2014/09/12 21:26:36	44°29.1′	6°39.9′	9.7	3.1	65	55	−20	37	0.59	0.04
2014/11/25 07:33:37	44°28.0′	6°40.5′	8.0	3.1	25	45	−70	36	0.55	0.07
2015/02/10 05:39:11	44°31.6′	6°38.9′	10.9	3.0	60	35	−30	31	0.65	0.02

Mainshocks in bold. NOBS, number of polarities; STDR, Station distribution ratio (> 0.5 means a more reliable mechanism); *F*, fit (0 = perfect fit; 1 = perfect misfit).

Tinée fault), and by Leclère *et al.* (2012) who proposed a hydrogeological flow model along similar northwest–southeast-striking faults. Taking into account the 70°SW dip of the fault plane, any link with local tectonics should rather be searched out in the northeastern part of the study area (Fig. 1). This is precisely where the Frontal Penninic Thrust, the main tectonic boundary of the region, is to be found with again a northwest–southeast strike. But it is primarily a northeast-dipping thrust fault, not a normal fault. The only clues of fracture in the study area are the numerous small faults first mapped in the Embrunais-Ubaye nappes themselves 50 years ago (Kerckhove, 1969; Kerckhove *et al.*, 2005). The foliated nature of the flysch, the rough topography, moraines and screes hiding accessible outcrops might anyway explain the difficulty to map faults and to ascertain their strikes. Figure 1 shows that, in the study area, most of these faults strike almost north–south (not N165°E); a very few ones have a southwest–northeast strike, and could explain the complexity of the swarm, where we observed such transverse lineaments, active for a few days before quickly dying down (Figs. 3 [right] and 6).

In the preceding paragraphs, the term "swarm" is hardly used because we mainly discussed the relation between the two largest events of the sequence. Clearly, the activity we observed over a 3.5 yr period does not abide by the Omori law as could be expected for M_L 4.3 and 4.8 shocks: it is basically swarm-like, but with a complexification brought by the two shocks of larger magnitude, each with their own foreshocks and aftershocks superimposing onto the swarm. EQ1 undoubtedly had foreshocks and aftershocks, and soon activated a swarm which slowly grew to a maximal length of 5.5 km, following a kind of diffusion law with a hydraulic diffusivity of 0.05 $m^2\ s^{-1}$ compatible with what had been observed in 2003–2004 (Fig. 8, top and middle). Whether EQ2 was preceded by foreshocks or not is a moot point. If it was followed by genuine aftershocks, it was for a short spell only, as shown by the remarkable want of $M_L \geq 3$ shocks over a 2 month period (Fig. 2). Quasi instantaneously, EQ2 mainly reactivated, without any diffusion process (Fig. 8, bottom), the entire swarm that had taken two years to reach its 5.5 km length. It also triggered activity up to 5.5 km to the northwest of the mainshock, which eventually made the whole swarm ~11 km long (Fig. 7).

Although swarms are common in Ubaye, they were never observed as protracted as the one under study. Curiously, there is a belief in this valley that earthquakes and flooding often coincide, and indeed the three largest earthquakes in the last 60 years occurred in springtime, namely: M_w 5.5 on 5 April 1959, M_L 4.3 on 26 February 2012, and M_L 4.8 on 7 April 2014. Rare cases of precipitation-induced seismicity have previously been reported in the central Alps (Roth *et al.*, 1992; Deichmann *et al.*, 2006) or in America (Saar and Manga, 2003), but there was in Ubaye no exceptional rainfall or snowmelt which could explain the late seismic activity (whereas flooding in 1957, 1963, 1989, 1997, 2002, and 2008 caused damage without being followed by any unusual seismicity). We therefore believe that the occurrence of these three shocks on different years between the end of February and the beginning of April is simply fortuitous.

For the local population, the most important questions were and still are: when will it stop and could it be worse? Without, of course, being able to meet this information demand, this article demonstrates that precise locations can help to construct diverse scenarios. Since 2003, the activity has clearly globally migrated towards the northwest, but this plain statement is actually much more complex since, within the 2003–2004 and the 2012–2015 swarms, migration was observed toward the southeast. If now the activity further propagates to the northwest where the tectonic context is pretty much the same (still beneath the Embrunais-Ubaye nappes), it does not necessarily mean that the rupture will steadily continue from the northwestern tip of the present swarm. Instead, the next swarm, possibly triggered by another "mainshock", could be located much farther to the

northwest. Its subsequent growth toward the southeast could, if not in-line with the present swarm, perhaps create another bayonet such as the one observed between the 2003–2004 and the 2012–2015 swarms (Fig. 3). Since the inception of the 2012 swarm, we have been intrigued by this bayonet, expecting it to give way to any subsequent event. There is still a possibility for a strike-slip earthquake with a magnitude up to 5 to occur there in the future. The gap that still exists in the north of the present swarm close to latitude 44°31′N also leaves room for another smaller-magnitude earthquake.

Gardner and Knopoff (1974) once stated that "approximately two-thirds of [earthquakes] were aftershocks". We guess that, if their window algorithm were applied to the Ubaye sequence, the catalog with aftershocks removed would be very light. What happened in Ubaye can in a way be compared with the 1997–1998 Colfiorito (Central Italy) swarm where two "mainshocks" (M_w 5.7 and 6.0) occurred the same day on the same structure (Barba and Basili, 2000), and were followed, some 20 days later, by another M_w 5.6 shock. But the first two "mainshocks" were 3.5 km apart and unilaterally ruptured two different fault segments, whereas the third one, 15 km away and bidirectional, extended the rupture by 8 km. Apart from the difference in magnitude and fault length, the Ubaye case studied here is peculiar because, within slightly more than two years, the same fault segment ruptured twice on patches situated at different depths. This triggered and reactivated a prolific and protracted seismic swarm, thus deeply intermingling mainshock and swarm sequences. Vidale and Shearer (2006) pointed out that the distinction between swarms and mainshock sequences is gradational; Anderson and Nanjo (2013) recently took up the same concept of which the Ubaye case can undoubtedly be considered a paragon. Without attempting to paraphrase Gardner and Knopoff (1974), we hypothesize that all earthquake sequences are swarms which sometimes, but perhaps not so frequently, present a classical foreshock–mainshock–aftershock pattern.

Data and Resources

The Windows 7 and Linux versions of PICKEV2015, a freeware for picking arrival times, locating earthquakes, and computing magnitudes developed by J. Fréchet and F. Thouvenot, can be downloaded from https://sismalp.osug.fr/ftp-sismalp/freeware (last accessed July 2016). The Windows 7 and Linux versions of HYPREF2015, a freeware based on HYPO71 (Lee and Lahr, 1975) for locating earthquakes and developed by J. Fréchet, can be downloaded from https://sismalp.osug.fr/ftp-sismalp/freeware (last accessed July 2016). The mp4 animation snapshots of Figure 6 are available on http://isterre.fr/Francois-Thouvenot,1061 (last accessed July 2016). All plots were made using Generic Mapping Tools version 3.4 (http://gmt.soest.hawaii.edu, last accessed August 2016; Wessel and Smith, 1998).

Acknowledgments

M. and Mme Bravo, and M. and Mme Stenger generously allowed us to install semipermanent seismic recorders in their homes, respectively, at Sainte-Anne (La Condamine-Châtelard) and Tournoux (Saint-Paul-sur-Ubaye). The Sismalp network was designed in 1987 by Julien Fréchet, Robert Guiguet, and the first two authors of this article; without the muscle, ingenuity, and commitment of J.F. and R.G., this network would never have been fully operational. Data from other seismic networks (namely Résif and LDG, France, and SED, Switzerland) were used when available, and we thank the relevant colleagues and technical staff. Felix Waldhauser helped us to tune input parameters in his hypoDD program. The Conseil général de l'Isère, the Délégation aux risques majeurs (French Ministry of the Environment), the Institut national des sciences de l'Univers (CNRS), and the Conseil régional Rhône-Alpes funded the Sismalp network. The Réseau national de surveillance sismique and several departmental councils (Isère, Alpes-de-Haute-Provence, Haute-Savoie, Hautes-Alpes, Ain, and Savoie) support its running costs.

References

Anderson, J. G., and K. Nanjo (2013). Distribution of earthquake cluster sizes in the western United States and in Japan, *Bull. Seismol. Soc. Am.* **103,** 412–423.

Barani, S., G. Ferretti, D. Scafidi, and D. Spallarossa (2014). Analysis of seismicity and micro-seismicity associated with the October–November 2010 Sampeyre swarm, Southwestern Alps, *Tectonophysics* **611,** 130–140.

Barba, S., and R. Basili (2000). Analysis of seismological and geological observations for moderate-size earthquakes: The Colfiorito Fault System (Central Apennines, Italy), *Geophys. J. Int.* **141,** 241–252.

Cara, M., Y. Cansi, A. Schlupp, P. Arroucau, N. Béthoux, É. Beucler, S. Bruno, M. Calvet, S. Chevrot, A. Deboissy, *et al.* (2015). SI-Hex: A new catalogue of instrumental seismicity for metropolitan France, *Bull. Soc. Géol. France* **186,** 3–19.

Courboulex, F., A. Dujardin, M. Vallée, B. Delouis, C. Sira, A. Deschamps, L. Honoré, and F. Thouvenot (2013). High-frequency directivity effect for an M_w 4.1 earthquake, widely felt by the population in southeastern France, *Bull. Seismol. Soc. Am.* **103,** doi: 10.1785/0120130073.

Daniel, G., E. Prono, F. Renard, F. Thouvenot, S. Hainzl, D. Marsan, A. Helmstetter, P. Traversa, J.-L. Got, L. Jenatton, *et al.* (2011). Changes in effective stress during the 2003-2004 Ubaye seismic swarm, France, *J. Geophys. Res.* **116,** no. B01309, doi: 10.1029/2010JB007551.

Deichmann, N., M. Baer, J. Braunmiller, S. Husen, D. Fäh, D. Giardini, P. Kästli, U. Kradolfer, and S. Wiemer (2006). Earthquakes in Switzerland and surrounding regions during 2005, *Eclogae Geol. Helv.* **99,** 443–452.

Fréchet, J. (1978). Sismicité du Sud-Est de la France, et une nouvelle méthode de zonage sismique, *Ph.D. Thesis*, Univ. Sci. Méd. Grenoble, France (in French).

Fréchet, J., and N. Pavoni (1979). Étude de la sismicité de la zone briançonnaise entre Pelvoux et Argentera (Alpes occidentales) à l'aide d'un réseau de stations portables, *Eclogae Geol. Helv.* **72,** 763–779 (in French).

Gardner, J. K., and L. Knopoff (1974). Is the sequence of earthquakes in southern California, with aftershocks removed, Poissonian? *Bull. Seismol. Soc. Am.* **64,** 1363–1367.

Guyoton, F., J. Fréchet, and F. Thouvenot (1990). La crise sismique de janvier 1989 en Haute-Ubaye (Alpes-de-Haute-Provence, France): étude fine de la sismicité par le nouveau réseau Sismalp, *C. R. Acad. Sci. Paris* **311,** 985–991 (in French).

Hainzl, S., and T. Fischer (2002). Indications for a successively triggered rupture growth underlying the 2000 earthquake swarm in Vogtland/NW Bohemia, *J. Geophys. Res.* **107,** no. B122338, doi: 10.1029/2002JB001865.

Horálek, J., and T. Fischer (2010). Intraplate earthquake swarms in West Bohemia/Vogtland (Central Europe), *Jökull* **60,** 67–87.

Jenatton, L., R. Guiguet, F. Thouvenot, and N. Daix (2007). The 16,000-event 2003-2004 earthquake swarm in Ubaye (French Alps), *J. Geophys. Res.* **112,** no. B11304, doi: 10.1029/2006JB004878.

Kerckhove, C. (1969). La "zone du Flysch" dans les nappes de l'Embrunais-Ubaye (Alpes occidentales), *Géologie Alpine* **45,** 5–204 (in French).

Kerckhove, C., J. Debelmas, and P. Cochonat (1978). Tectonique du soubassement parautochtone des nappes de l'Embrunais-Ubaye sur leur bordure occidentale, du Drac au Verdon, *Géologie Alpine* **54,** 67–82 (in French).

Kerckhove, C., M. Gidon, and J.-L. Pairis (2005). Carte géol. France (1/50 000), feuille Embrun-Guillestre (871), BRGM, Orléans (in French).

Knett, J. (1899). Das Erzgebirgische Schwarmbeben zu Hartenberg vom 1. Jänner bis Feber 1824, *Sitzungsber. Deutsch. Naturwiss.-Med. Ver. Böhmen* **19,** 167–191 (in German).

Leclère, H., G. Daniel, O. Fabbri, F. Cappa, and F. Thouvenot (2013). Tracking fluid pressure build-up from focal mechanisms during the 2003–2004 Ubaye seismic swarm, *J. Geophys. Res.* **118,** 4461–4476.

Leclère, H., O. Fabbri, G. Daniel, and F. Cappa (2012). Reactivation of a strike-slip fault by fluid overpressuring in the southwestern French-Italian Alps, *Geophys. J. Int.* **189,** no. 1, 29–37, doi: 10.1111/j.1365-246X.2011.05345.x.

Lee, W. H. K., and J. E. Lahr (1975). hypo71: A computer program for determining hypocenter, magnitude, and first-motion pattern of local earthquakes, *U.S. Geol. Surv. Open-File Rept. 75-331*, 110 pp.

Reasenberg, P. A., and D. H. Oppenheimer (1985). fpfit, fpplot and fppage: fortran computer programs for calculating and displaying earthquake fault plane solutions, *U.S. Geol. Surv. Open-File Rept. 85-739*, 109 pp.

Roth, P., N. Pavoni, and N. Deichmann (1992). Seismotectonics of the eastern Swiss Alps and evidence for precipitation-induced variations of seismic activity, *Tectonophysics* **207,** 183–197.

Saar, M., and M. Manga (2003). Seismicity induced by seasonal groundwater recharge at Mt Hood, Oregon, *Earth Planet. Sci. Lett.* **214,** 505–618.

Sanchez, G., Y. Rolland, D. Schreiber, G. Giannerini, M. Corsini, and J.-M. Lardeaux (2010). The active fault system of the SW Alps, *J. Geodyn.* **49,** no. 5, 296–302, doi: 10.1016/j.jog.2009.11.009.

Scafidi, D., S. Barani, R. De Ferrari, G. Ferretti, M. Pasta, M. Pavan, D. Spallarossa, and C. Turino (2015). Seismicity of Northwestern Italy during the last 30 years, *J. Seismol.* **19,** 201–218.

Sellami, S., E. Kissling, F. Thouvenot, and J. Fréchet (1995). Initial reference velocity model for seismic tomography in the western Alps, *20th Gen. Ass. Europ. Geophys. Soc.*, Hamburg.

Shapiro, S. A., E. Rothert, V. Rath, and J. Rindschwentner (2002). Characterization of fluid transport properties of reservoirs using induced microseismicity, *Geophysics* **67,** 112–220.

Sira, C., A. Schlupp, M. Schaming, C. Chesnais, C. Cornou, A. Dechamp, E. Delavaud, and E. Maufroy (2014). Séisme de Barcelonnette du 7 avril 2014, *Rapport BCSF2014-R1*, 76 pp. (in French).

Sira, C., A. Schlupp, M. Schaming, and M. Granet (2012). Séisme de Barcelonnette du 26 février 2012, *Rapport BCSF2012-R1*, 43 pp. (in French).

Špičák, A. (2000). Earthquake swarms and accompanying phenomena in intraplate regions: A review, *Studia geoph. et geod.* **44,** 89–106.

Sue, C. (1998). Dynamique actuelle et récente des Alpes occidentales internes– Approches structurale et sismologique, *Ph.D. Thesis*, Univ. J. Fourier, Grenoble, France (in French).

Sue, C., F. Thouvenot, J. Fréchet, and P. Tricart (1999). Widespread extension in the core of the western Alps revealed by earthquake analysis, *J. Geophys. Res.* **104,** 25,611–25,622.

Thouvenot, F., and J. Fréchet (2006). Seismicity along the north-western edge of the Adria microplate, in *The Adria Microplate: GPS Geodesy, Tectonics, and Hazards*, N. Pinter, G. Grenerczy, J. Weber, S. Stein, and D. Medak (Editors), Springer, Dordrecht, 100–120.

Vidale, J. E., and P. M. Shearer (2006). A survey of 71 earthquake bursts across South California exploring the role of pore fluid pressure fluctuation and aseismic slip as drivers, *J. Geophys. Res.* **111,** no. B05312, doi: 10.1029/2005JB004034.

Waldhauser, F. (2001). hypodd: A program to compute double-difference hypocenter locations, *U.S. Geol. Surv. Open-File Rept. 01-113*, 25 pp.

Waldhauser, F., and W. L. Ellsworth (2000). A double-difference earthquake location algorithm: Method and application to the Northern Hayward Fault, California, *Bull. Seismol. Soc. Am.* **90,** 1353–1368.

Wessel, P., and W. H. F. Smith (1998). New, improved version of Generic Mapping Tools released, *Eos Trans. AGU* **79,** 579.

Université Grenoble Alpes/CNRS/ISTerre
CS 40700
38058 Grenoble Cedex 09
France
thouve@ujf-grenoble.fr
liliane.jenatton@laposte.net
bertrand.potin@univ-grenoble-alpes.fr
(F.T., L.J., B.P.)

Università di Genova/DISTAV
5 viale Benedetto XV
16132 Genova
Italy
scafidi@dipteris.unige.it
turino@dipteris.unige.it
ferretti@dipteris.unige.it
(D.S., C.T., G.F.)

Manuscript received 15 September 2015;
Published Online 13 September 2016